Title
Anomalous Flattening of the Fast-Ion Profile during Alfvén-Eigenmode Activity

Journal
Physical Review Letters, 99(24)

ISSN
0031-9007

Authors
Heidbrink, WW
Gorelenkov, NN
Luo, Y
et al.

Publication Date
2007-12-14

DOI
10.1103/physrevlett.99.245002

Anomalous Flattening of the Fast-Ion Profile during Alfvén-Eigenmode Activity

W. W. Heidbrink,[1] N. N. Gorelenkov,[2] Y. Luo,[1] M. A. Van Zeeland,[3] R. B. White,[2] M. E. Austin,[4] K. H. Burrell,[3] G. J. Kramer,[2] M. A. Makowski,[5] G. R. McKee,[6] R. Nazikian,[2] and the DIII-D team

[1]*University of California, Irvine, California 92697, USA*
[2]*Princeton Plasma Physics Laboratory, Princeton, New Jersey 08543, USA*
[3]*General Atomics, P.O. Box 85608, San Diego, California 92186-5608, USA*
[4]*University of Texas, Austin, Texas 78712-0263, USA*
[5]*Lawrence Livermore National Laboratory, Livermore, California 94550, USA*
[6]*University of Wisconsin, Madison, Wisconsin 53706, USA*

(Received 29 June 2007; published 12 December 2007)

Neutral-beam injection into plasmas with negative central shear produces a rich spectrum of toroidicity-induced and reversed-shear Alfvén eigenmodes in the DIII-D tokamak. The first application of fast-ion D_α (FIDA) spectroscopy to Alfvén-eigenmode physics shows that the central fast-ion profile is anomalously flat in the inner half of the discharge. Neutron and equilibrium measurements corroborate the FIDA data. The current density driven by fast ions is also strongly modified. Calculations based on the measured mode amplitudes do not explain the observed fast-ion transport.

DOI: 10.1103/PhysRevLett.99.245002 PACS numbers: 52.55.Pi, 52.35.Bj, 52.55.Fa

α particles produced in deuterium-tritium fusion reactions may drive Alfvén eigenmodes [1,2] unstable in ITER and other burning plasma experiments. If they do, the most important practical issue is the resultant fast-ion transport. Will benign local flattening of the α-particle pressure profile occur? Or will the α particles escape from the plasma and damage the first wall? The expulsion of fast ions by toroidicity-induced Alfvén eigenmodes (TAE) has damaged internal vessel components in two tokamaks [3,4]. The damage was explained qualitatively in terms of wave-particle resonances and orbital effects, but no quantitative comparisons between the measured fluctuation levels and the expected transport were given in these publications. In the only quantitative studies of this important issue [5,6], wave amplitudes an order of magnitude larger than the measured values were needed to predict the large losses observed experimentally.

The fast-ion and instability diagnostics were coarse in these early studies, suggesting that misinterpretation of the available signals might account for the discrepancy. In the work reported here, however, both the instabilities and the fast-ion response are very well characterized. Nevertheless, the calculated fast-ion transport is still much smaller than the observed value.

The DIII-D tokamak has an extensive suite of fluctuation diagnostics with the bandwidth and sensitivity needed to detect Alfvén instabilities. A 40-channel electron cyclotron emission (ECE) diagnostic measures electron temperature (T_e) fluctuations, density (n_e) fluctuations are measured by reflectometry, beam-emission spectroscopy, and CO_2 interferometry and magnetic fluctuations are measured by Mirnov coils. A detailed comparison of these measurements with the mode structures predicted by linear ideal MHD theory was recently reported [7]. Both the electron temperature and the electron density eigenfunctions are in excellent agreement with the NOVA code [8] for the $n = 3$ TAE and the reversed-shear Alfvén eigenmode (RSAE). (n is the toroidal mode number.) This Letter documents the fast-ion response to these well-characterized wave fields.

In the baseline discharge (no. 122117) [7], 4.6 MW of 80-keV deuterium neutral beams are injected in the direction of the plasma current into a low-density ($\bar{n}_e = 2 \times 10^{13}$ cm^{-3}), magnetically diverted, deuterium plasma with central $T_e = 1$–2 keV. The beams are injected early in the current ramp to produce a reversed-shear plasma with an off-axis minimum in the safety factor q at $\rho_{q\,\mathrm{min}}$. (The normalized minor radius coordinate is proportional to the square root of the toroidal flux ρ.) The central beam pressure is large ($\sim 50\%$ of the total), and the ratio of the injected beam speed to the Alfvén speed is ~ 0.45. At the magnetic axis, the peak of the fast-ion distribution function occurs at a pitch of $v_\parallel/v = 0.68$.

The fast-ion response to the instabilities is determined by four independent techniques. The primary diagnostic is a new charge-exchange recombination spectroscopy technique that utilizes the Doppler-shifted Balmer-α light emitted by fast ions [9,10]. Beam modulation and fitting of impurity lines is used to extract the fast-ion spectra from the interfering background light [10]; uncertainties in background subtraction are the dominant source of error and are represented by error bars in the figures. In this Letter, the spectra from this fast-ion D_α (FIDA) diagnostic are averaged over wavelengths that correspond to energies along the vertical line of sight of $E_\lambda = 30$–60 keV. The wavelength-integrated signals are divided by the injected neutral density to yield fast-ion density measurements in most of the high-energy portion of velocity space [11] with a spatial resolution of a few centimeters. The second diagnostic is the volume-averaged deuterium-deuterium neutron rate S_n. Under these conditions, S_n is dominated

by beam-plasma reactions between the fast and thermal populations, so the signal is proportional to the number of high-energy fast ions in the plasma. To detect effects caused by the instabilities, the signal is normalized to the classically expected rate due to collisional processes (as calculated by TRANSP [12]). The third diagnostic relies on motional Stark effect (MSE) measurements of the internal magnetic field. The profile of the total plasma pressure is obtained from EFIT [13] reconstructions of the MHD equilibrium that are consistent with the MSE and magnetics data and with isotherms of the electron temperature. The thermal pressure from T_e, n_e, T_i, and carbon density measurements (the dominant impurity) is subtracted from the MHD pressure profile to obtain the fast-ion pressure p_f. The absolute uncertainty in the inferred fast-ion pressure at $\rho = 0.25$ is $\sim$16% and the relative uncertainty is $\sim$8%. In the fourth technique, the evolution of the q profile provides information on the neutral-beam current drive (NBCD) profile, which is sensitive to the spatial profile of circulating fast ions. In addition to the evolution of $q_{\min}$ inferred from the equilibrium reconstructions, rational values of $q_{\min}$ are also inferred from the temporal pattern of frequency-sweeping RSAEs with different toroidal mode numbers [2].

Strong Alfvén activity occurs early in the discharge [Fig. 1(a)]. RSAEs that are localized near $\rho_{q\,\min}$ and more global TAEs are both observed [7]. When the frequency of a RSAE sweeps across a TAE frequency, the eigenfunctions mix. Throughout the period of strong activity, both the neutron rate and the FIDA density are suppressed relative to their classically expected values [Fig. 1(b)]. The magnitude of this suppression correlates with the amplitude of the mode activity. Figure 2 shows data from five similar discharges with different values of beam power. Because of the complexity of the Alfvén activity, it is difficult to quantify the composite amplitude. Figure 2 uses the amplitude of the ten strongest modes as measured by ECE; the correlation is similar using a bandpass-filtered Mirnov signal. These results strongly suggest that the observed reductions in the fast-ion signal are caused by the Alfvén activity.

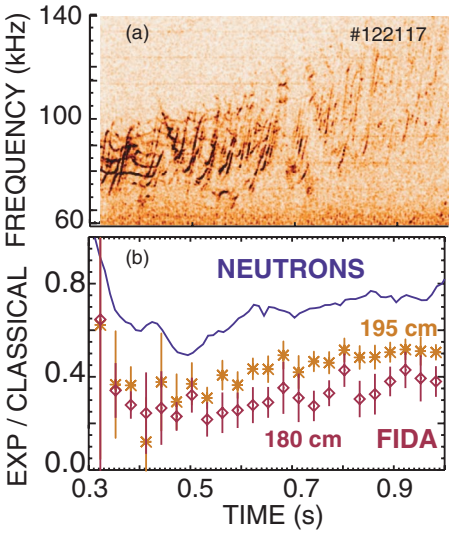

FIG. 1 (color online). (a) Cross power of radial and vertical CO_2 interferometer channels showing the many RSAEs (upward-sweeping lines) and TAEs ($\sim$ horizontal lines) in the plasma. (b) Neutron rate and FIDA densities at $R = 180$ and 195 cm vs time. The signals are normalized by the classical TRANSP neutron and beam-ion density predictions, respectively. The absolute calibrations of the neutron and FIDA data are adjusted so that the ratio is unity in the preceding 2.3 MW discharge at 2.0 s (when the Alfvén activity is undetectable).

The Alfvén activity flattens the fast-ion spatial profile. Both the FIDA density profile and the fast-ion pressure profile from MSE are much flatter during the strongest activity than they are later in the discharge (Fig. 3). Although the pressure profile peaks as the activity weakens, it is still less peaked than classically expected at 1.2 s. This is in contrast to the profiles observed in MHD-quiescent plasmas, which are in excellent agreement with the TRANSP predictions [14].

The FIDA spectrum is sensitive to the perpendicular energy distribution [14]; distorted spectra are sometimes observed during Alfvén activity and are common during ion cyclotron heating [11]. In discharge no. 122117, however, the spectra agree (within the uncertainties) with the spectral shape normally observed in quiet plasmas. This suggests that the transport process changes the average perpendicular energy of the fast ions no more than $\sim$5 keV.

In the presence of this fast-ion transport, the plasma current diffuses more gradually than classically predicted [Fig. 4(a)]. Two independent measurements of the evolution of $q_{\min}$ are in excellent agreement. They differ markedly from the classical predictions calculated by special TRANSP simulations that begin with the measured equilibrium, then evolve the current profile assuming neoclassical

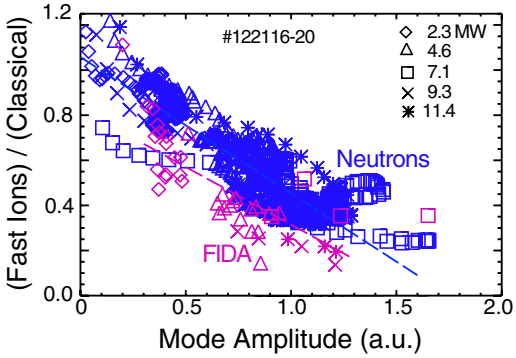

FIG. 2 (color online). Normalized neutron rate and $R = 180$ cm FIDA density versus approximate mode amplitude at various times in five successive discharges with increasing amounts of beam power. The dashed lines are linear fits to the data.

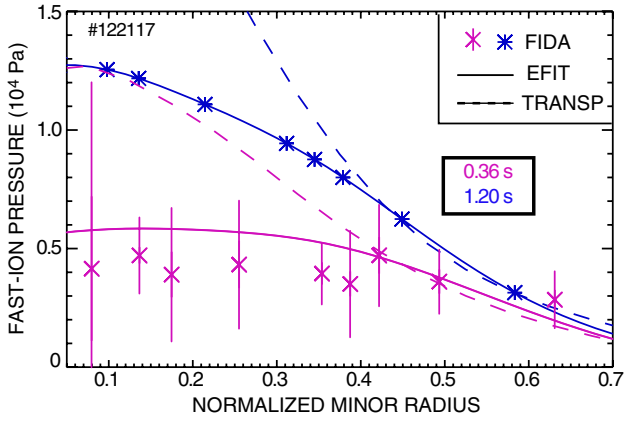

FIG. 3 (color online). Fast-ion pressure profiles and FIDA density profiles versus ρ at two different times that correspond to normalized neutron rates of 0.66 and 0.94. The dashed lines are the classical pressure profile predicted by TRANSP. The FIDA density profile is normalized to the MSE-EFIT p_f profile at 1.2 s.

flux diffusion. These simulations adjust the boundary value of the parallel electric field to match the measured plasma current. For either of two extreme assumptions—either classical NBCD or no NBCD whatsoever—the predicted diffusion is far more rapid than experimentally observed. Evidently, both the classical NBCD profile and the neoclassical conductivity profile are more peaked than the actual current profile. A simulation that uses the NBCD expected from a centrally flattened fast-ion density profile is in better agreement with experiment. Gradual evolution

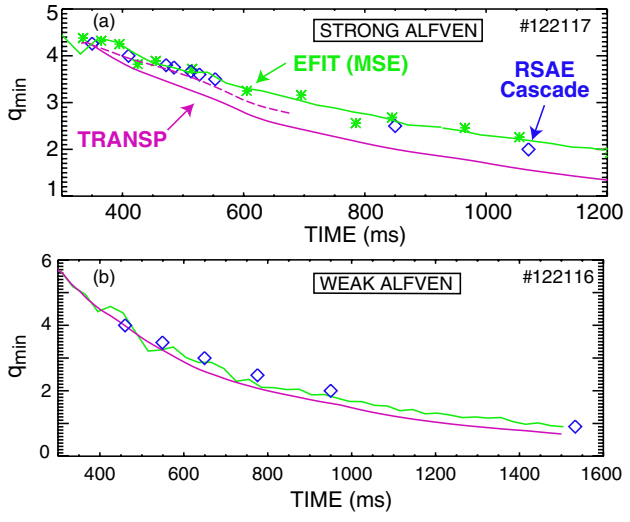

FIG. 4 (color online). Measured evolution of $q_{\min}$ from MSE-based equilibrium reconstructions (line) and RSAE rational integer crossings (diamond) in discharges with (a) strong Alfvén activity (4.6 MW) and (b) weak Alfvén activity (2.3 MW). The TRANSP simulations assume either classical NBCD (solid line) or the NBCD from a centrally flattened fast-ion density profile (dashed line).

of $q_{\min}$ was previously reported [15] in more poorly diagnosed discharges. In contrast, in the discharge with lower beam power and much weaker Alfvén activity, the current evolution is close to the classical expectation [Fig. 4(b)].

The strongest modes in the spectrum [Fig. 1(a)] have peak internal magnetic perturbations of $\delta B_r/B \lesssim \times 10^{-3}$. Published theoretical simulations of fast-ion transport often require larger amplitudes than this to obtain significant transport; see, e.g., Refs. [5,6,16]. To determine if the measured Alfvén activity can explain the observed fast-ion transport, the 11 strongest toroidal modes are matched to NOVA linear eigenfunctions and the amplitudes are scaled to agree with the ECE measurements. Reliable mode identification is possible for the largest 7–8 modes but is problematic for the weakest ones or for modes with similar frequencies. For each toroidal mode, the strongest poloidal harmonics m are selected and a total of 151 (n, m) helical perturbations with their experimental amplitudes and frequencies are entered into the Hamiltonian guiding center code ORBIT [17]. Shear Alfvén waves with weak kinetic effects are assumed ($\delta E_\parallel = \delta B_\parallel = 0$), so the transport caused by parallel electric and magnetic wave fields is neglected. Evolution of the frequency and mode structure is ignored since these barely change on orbital time scales. The initial fast-ion birth distribution function F_0 is taken from TRANSP. The particle orbits are computed in the presence of pitch-angle scattering and the perturbed fields, then the distribution function F is sampled for comparison with F_0.

This procedure cannot account for the observed fast-ion transport. Figure 5 shows the change in the distribution function in the region of velocity space that makes the dominant contribution to the measured fast-ion signals for ORBIT runs where the mode amplitudes are artificially

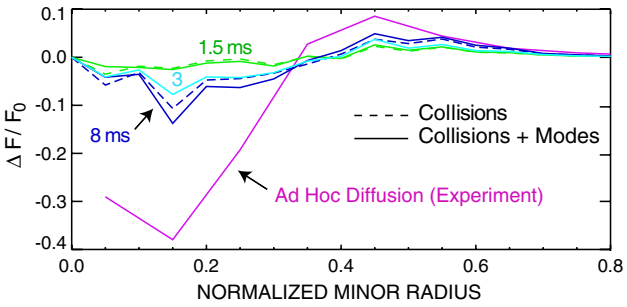

FIG. 5 (color online). Change in the distribution function of fast ions with $E \geq 60$ keV and $v_\parallel/v = 0.4$–0.7 vs ρ; ΔF is normalized to the maximum value of the initial distribution function. The dashed lines are with collisions alone; the solid lines include collisions and 151 helical modes at 5 times the experimental amplitudes for the TAEs and RSAEs that are observed at 356 ms. The distribution function is sampled after 0.95–1.9 ms (green), 1.9–3.8 ms (turquoise), and 5.5–11 ms (purple). The (red) curve compares a TRANSP simulation with $D_B = 5$ m^2/s inside $\rho = 0.55$ and zero outside with a standard ($D_B = 0$) simulation.

enhanced by a factor of 5. Even with this enormous enhancement, which is much larger than the experimental uncertainty of $\lesssim 10\%$, the transport is smaller than observed. To estimate the experimental transport, an *ad hoc* diffusion coefficient D_B is employed in a sequence of special TRANSP runs that hold all other plasma parameters fixed. Spatially variable diffusion that is very large ($\gtrsim 5$ m^2/s) inside $\rho \simeq 0.55$ and tiny outside is needed for consistency with the measured FIDA and p_f profiles. The ORBIT simulations predict transport in the correct locations but, even with 5 times the measured amplitude, the change in the distribution function is far too small. The predicted transport is comparable to neoclassical diffusion.

The ORBIT simulation uses the strongest modes observed experimentally at a single representative time. However, many weaker intermittent modes appear at lower frequencies; perhaps these play an important role in the observed transport. (Neoclassical tearing modes are absent.)

In summary, four independent diagnostics all indicate strong transport of fast ions in reversed-shear discharges with multiple TAE and RSAE modes that have $\delta B_r/B \lesssim O(10^{-3})$. In quiet plasmas, these same diagnostics agree with classical [14] and ion cyclotron [11] theory. Moreover, similar profiles are measured with different techniques during Alfvén activity on JT-60U [18]. The mode amplitudes are also measured by four independent diagnostics [7]. The hypothesis that diagnostic inadequacies account for the discrepancy between theory and experiment is therefore excluded. Fast-ion transport is remarkably effective in plasmas with Alfvén activity. Identification of the mechanism responsible for this transport is an urgent task in burning plasma physics.

This work was funded by U.S. DOE Subcontract No. SC-G903402 to U.S. DOE Contracts No. DE-FC02-04ER54698, No. DE-AC02-76CHO3073, No. DE-FG03-97ER54415, No. W-7405-ENG-48, and No. DE-FG02-89ER53296.

[1] C. Z. Cheng, L. Chen, and M. Chance, Ann. Phys. (N.Y.) **161**, 21 (1985).
[2] S. E. Sharapov *et al.*, Phys. Plasmas **9**, 2027 (2002).
[3] H. H. Duong *et al.*, Nucl. Fusion **33**, 749 (1993).
[4] R. B. White *et al.*, Phys. Plasmas **2**, 2871 (1995).
[5] E. M. Carolipio *et al.*, Phys. Plasmas **8**, 3391 (2001).
[6] Y. Todo *et al.*, Phys. Plasmas **10**, 2888 (2003).
[7] M. A. Van Zeeland *et al.*, Phys. Rev. Lett. **97**, 135001 (2006); Phys. Plasmas **14**, 056102 (2007).
[8] C. Z. Cheng, Phys. Rep. **1**, 211 (1992).
[9] W. W. Heidbrink *et al.*, Plasma Phys. Controlled Fusion **46**, 1855 (2004).
[10] Y. Luo *et al.*, Rev. Sci. Instrum. **78**, 033505 (2007).
[11] W. W. Heidbrink *et al.*, Plasma Phys. Controlled Fusion **49**, 1457 (2007).
[12] R. V. Budny, Nucl. Fusion **34**, 1247 (1994).
[13] L. L. Lao *et al.*, Nucl. Fusion **25**, 1611 (1985).
[14] Y. Luo *et al.*, Phys. Plasmas **14**, 112503 (2007).
[15] K. L. Wong *et al.*, Phys. Rev. Lett. **93**, 085002 (2004).
[16] D. J. Sigmar *et al.*, Phys. Fluids B **4**, 1506 (1992).
[17] R. B. White and M. S. Chance, Phys. Fluids **27**, 2455 (1984).
[18] M. Ishikawa *et al.*, Nucl. Fusion **47**, 849 (2007).